Materials Science & Engineering A 683 (2017) 94–102

Contents lists available at ScienceDirect

Materials Science & Engineering A

journal homepage: www.elsevier.com/locate/msea

Evolution of texture and microstructure during high strain rate torsion of aluminium zinc magnesium copper alloy

Shailesh Tiwari[a], Sumeet Mishra[b], A. Odeshi[c], J.A. Szpunar[c], Manoj Chopkar[a,*]

[a] Department of Metallurgical Engineering, National Institute of Technology Raipur, Raipur 492010, India
[b] Department of Materials Science and Engineering, Indian Institute of Technology Kanpur, Kanpur 208016, India
[c] Department of Mechanical Engineering, University of Saskatchewan, Saskatoon, SK, Canada S7N5C5

ARTICLE INFO

Keywords:
Strain rate
Torsion
Texture
Microstructure
Dynamic recovery

ABSTRACT

Deformation behaviour of aluminium-zinc-magnesium-copper alloy AA 7075 was investigated at high strain rate using Split Hopkinson Torsional Bar (SHTB). Cylindrical AA 7075 specimens were deformed at different angles of twist, giving rise to strain rate ranging from 700 s^{-1} to 2000 s^{-1}. Comprehensive microstructural and textural investigation was carried out using electron back scatter diffraction (EBSD), X-ray line profile analysis and bulk texture measurement using X-rays for all the deformed samples. The high strain rate torsion tested samples showed a characteristic torsion texture for face centre cubic materials with a dominant A $\{1\bar{1}\bar{1}\}<110>/\{\bar{1}11\}<\bar{1}\bar{1}0>$ component and the overall texture weakened with increase in strain rate and strain. Intragranular misorientation parameters like local average misorientation and grain orientation spread indicated occurrence of dynamic recovery in the sample deformed at the highest strain rate which was characterized by the maximum fraction of low angle grain boundaries. Microstructural parameters determined from X-ray diffraction using modified Williamson-Hall and Variance method further corroborated these results indicating the onset of dynamic recovery at the highest strain rate.

1. Introduction

AA 7075 has been the standard workhorse alloy in the aerospace industries since its inception in the year 1943 by Japanese company Sumitomo metal, [1]. An enviable combination of high mechanical strength, good fatigue resistance and adequate machinability makes this Al-Zn-Mg-Cu alloy a suitable option for aerospace applications like aircraft fittings, gears and shafts and other structural components [2]. The high strength to weight ratio of Al-Zn-Mg-Cu alloys can be attributed to interaction between mobile dislocations and finely dispersed precipitates [3]. However, these aircraft components are susceptible to dynamic impact loading in service, in which case strain rate of the order of ~10^3 s^{-1} can be achieved [4]. Such high strain rates can be achieved in the event of collision with flying debris or birds [4]. Consequently, catastrophic failure can occur or can cause severe maintenance and repair costs. Thus, it is of paramount importance to understand the deformation behaviour of Al-Zn-Mg-Cu alloys under dynamic loading conditions.

By and large, most of the investigations concerned with high strain rate deformation have been carried out using Split Hopkinson Pressure bar in compression mode [5–7]. During high strain rate compression, localized plastic deformation occurs due to adiabatic heating of the material [8]. This adiabatic heating of the material occurs along narrow paths of size ~ 5–100 µm [8]. Under quasi-static deformation, flow strength of the material increases with increasing reduction [9]. However, the formation of adiabatic shear bands during dynamic deformation causes a cascading effect that leads to accommodation of plastic deformation in these non crystallographic shear bands instead of conventional slip and aids in plastic deformation [10]. This is a calamitous effect which inevitably leads to failure. In addition, some authors have also reported the occurrence of continuous dynamic recrystallization and geometric dynamic recrystallization in the material due to adiabatic temperature rise during high strain rate deformation [11]. Therefore, in the recent years many investigations have been carried out to understand the micro-mechanism behind the formation of adiabatic shear bands [12,13].

Odeshi et al. [14] studied the effect of temper condition on quasi-static and dynamic response of age hardenable AA 2099 and AA 6061 alloys. AA 2099 showed better mechanical properties than AA 6061 under quasi-static loading, while a reverse behaviour was observed under dynamic loading. However, both the samples failed due to formation of adiabatic shear bands at high strain rate.

* Corresponding author.
E-mail address: mchopkar.met@nitrr.ac.in (M. Chopkar).

http://dx.doi.org/10.1016/j.msea.2016.11.105
Received 14 October 2016; Received in revised form 29 November 2016; Accepted 30 November 2016
Available online 01 December 2016
0921-5093/

Microstructural characterization revealed that the temper condition plays an important role in formation of shear bands under dynamic loading conditions [14]. In addition, dissolution of second phase particles within the shear bands was also observed [14]. Since the second phase particles act as barriers to dislocation motion, dissolution of these particles led to reduction in deformation resistance and localization of shear strain.

Gurao et al. [11] carried out electron back scatter diffraction and bulk texture measurements to characterize the heterogeneous microstructure of impacted Al-Li alloy at different length scales. The shear bands contained fine sub-micron grains of the matrix phase and small spherical precipitates, while the region away from the shear band contained deformed and elongated grains. The unique deformation features observed at the interface between shear bands and rest of the sample was attributed to occurrence of continuous dynamic recrystallization and geometric dynamic recrystallization [11]. The presence of < 100 > oriented grains within the shear bands confirmed the fact that geometric dynamic recrystallization has occurred, while the wavy interface between the shear bands and rest of the sample indicated the occurrence of continuous dynamic recrystallization [11].

A few investigations focussing on texture evolution during high strain rate deformation have also been carried out [15,16]. Since the choice of slip systems in FCC materials is not sensitive to strain rate, the effect of strain rate on deformation texture was thought to be minimal [15]. However, few contradictory observations by Leffers et al. [17] and Bhattacharyya et al. [18,19] showed that depending upon temperature and strain rate, a specific deformation texture can be obtained. Bhattacharyya et al. [18,19] showed significant change in texture at high strain rates for copper, while no such differences were observed for iron. This was attributed to high strain hardening exponent (n) for copper (0.5) compared to iron (0.25). They proposed that higher strain hardening exponent of copper resulted in restricted grain rotations and in process altering the overall texture [18,19].

The effect of stacking fault energy on deformation texture at high strain rate was also analyzed and it was observed that the role of stacking fault energy is insignificant at high strain rate [20]. It was also observed that for samples deformed at high strain rate, deformation texture is relatively weak compared to samples deformed at nominal strain rates [20]. Canova et al. [21] proposed that at higher strain rates, rate sensitivity of slip increases causing the number of active slip systems to increase. Therefore, the plastic spin during deformation reduces causing a weak texture evolution [21]. A considerable amount of grain fragmentation was also observed in FCC metals and alloys at high strain rate deformation [20].

As evident from the above discussion, there is abundant literature available for high strain rate deformation under compression loading, while the same under torsion is scarce.

Therefore, in the present investigation, split Hopkinson torsional bar has been used to decipher deformation behaviour of Al-Zn-Mg-Cu alloys at a variety of strain rates ranging from 700 s^{-1} to 2000 s^{-1}. The deformed microstructures were characterized using bulk texture measurements, X-ray line profile analysis and electron back scatter diffraction to understand and appreciate the operative micro-mechanisms of deformation.

2. Experimental details

In the present investigation, extruded bars of diameter 30 mm of AA 7075 aluminium alloy were procured from Kaiser Aluminium, USA in T651 temper. The composition of the alloy determined using optical emission spectroscopy (OES) is given in Table 1.

The initial material was machined along extrusion direction to produce hollow cylindrical samples, as depicted in Fig. 1. The gage length is 3.8 mm, with an outer wall diameter of 13.8 mm and inner wall diameter of 13 mm resulting in wall thickness of 0.4 mm.

The split Hopkinson torsional bar consists of two elastic bars, a clamp with a sudden releasing mechanism, and a loading arrangement to twist one of the bars [22]. The hollow cylindrical sample is placed between the bars and twist is applied at one end of the bar via a loading mechanism [22]. This results in storage of torque between loading end of the bar and clamp. Subsequently, the sudden release of clamp results in propagation of shear stress pulse along the bar, thereby loading the sample in shear at high strain rate [22]. The different angles of twist used in the present investigation are 4, 10 and 16 degrees. The elastic wave data is acquired by oscilloscope connected to the strain gages mounted on both incident and transmitted bars. The elastic wave data is used to obtain stress strain and strain rate values for each test.

Table 1
Chemical composition of AA 7075.

Elements	Si	Fe	Cu	Mn	Mg	Cr	Zn	Ti	Al
wt%	0.12	0.25	1.6	0.06	2.6	0.2	5.8	0.07	Bal.

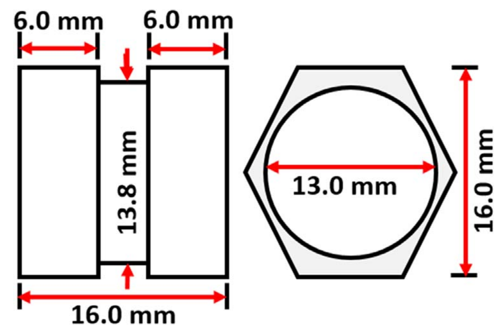

Fig. 1. Dimensions of the split Hopkinson torsional bar specimen.

Microstructural analysis was carried out using a JEOL field emission gun scanning electron microscope (FE-SEM) equipped with electron back scatter diffraction (EBSD) set up from Oxford instruments. The samples for EBSD were prepared via electropolishing using Struer's A2 electrolyte. Large area maps were captured with a step size 0.5 µm to ensure statistically significant data. HKL channel version 5.11 software was used for analyzing the EBSD data. Transmission electron microscopy (TEM) was carried out using Tecnai G^2 microscope operating at 200 kV. The samples for TEM were prepared via twin-jet electropolishing. A solution of 70% methanol and 30% nitric acid was used as electrolyte. Rigaku four circle goniometer was used to measure incomplete (111), (200), (220) and (311) pole figures with a maximum tilt angle of 70°. M-TEX, an open source software package for texture analysis was used to calculate the complete orientation distribution function (ODF) from incomplete pole figures. The ODF's were then used to calculate the complete pole figures. X-ray diffractograms for line profile analysis were captured using Rigaku Miniflex 600. Si powder was used as standard to separate the broadening contribution from instrument.

3. Data analysis

The elastic wave data captured by the stain gages mounted on the incident and transmitted bar were used to determine the average strain rate ($\dot{\gamma_s}$) using equation 1 [23].

$$\dot{\gamma_s}(t)=\frac{C_s D_s}{L_s D} * [\gamma_I(t)-\gamma_R(t)-\gamma_T(t)] \tag{1}$$

where, L_s and D_s are mean gage length and diameter of the sample, D is the diameter of the bar (25.4 mm), C_s is the shear wave velocity in the bar (3040 m/s) and$\gamma_I(t)$, $\gamma_R(t)$ and $\gamma_T(t)$ are the incident, reflected and transmitted strains, respectively. Eq. (1) can be integrated to obtain strain in the sample as a function of time.

The shear stress (τ_s) in the sample can be calculated from the stress